PERGAMON

Control Engineering Practice 10 (2002) 773–781

CONTROL ENGINEERING PRACTICE

www.elsevier.com/locate/conengprac

High-performance servo systems based on multirate sampling control ☆

Hiroshi Fujimoto[a,*], Yoichi Hori[b]

[a] Department of Electrical Engineering, Nagaoka University of Technology, Nagaoka, 940-2188, Japan
[b] Department of Electrical Engineering, The University of Tokyo, Tokyo, 113-8656, Japan

Received 26 May 2001; accepted 16 October 2001

Abstract

In this paper, novel multirate two-degree-of-freedom controllers are proposed for digital control systems, in which the sampling period of plant output is restricted to be relatively longer than the control period of plant input. The proposed feedforward controller assures perfect tracking at M inter-sampling points. On the other hand, the proposed feedback controller assures perfect disturbance rejection at M inter-sample points in the steady state. Illustrative examples of position control for hard disk drive are presented, and the advantages of these approaches are demonstrated.

Keywords: Multirate sampling control; Servo system; Tracking control; Disturbance rejection; Hard disk drive

1. Introduction

A digital control system usually has two samplers for the reference signal $r(t)$ and the output $y(t)$, and one holder on the input $u(t)$ as shown in Fig. 1. Therefore, there exist three time periods T_r, T_y, and T_u which represent the period of $r(t), y(t)$, and $u(t)$, respectively. The input period T_u is generally decided by the speed of the actuator, D/A converter, or the calculations on the CPU. On the other hand, the output period T_y is also determined by the speed of the sensor or the A/D converter.

Actual control systems usually hold the restrictions on T_u and/or T_y. Thus, in the conventional digital control systems, these three periods are made equal to the longer of the two periods T_u and T_y. However, multirate sampling control have been studied from the point of view of both control theories and applications (Araki, 1993). Authors also have developed some multirate sampling controllers, and applied them to motion control systems (Fujimoto, Kawamura, & Tomizuka, 1999a; Fujimoto, Hori, & Kawamura, 2001; Fujimoto, 2000).

In this paper, the digital control systems which have hardware restrictions of $T_u < T_y$ are assumed, and novel design methods of multirate two-degree-of-freedom (TDOF) controllers are proposed, which achieve "perfect tracking" and "perfect disturbance rejection" at M inter-sample points in T_y. The restriction of $T_u < T_y$ may be general because D/A converters are usually faster than the A/D converters. Especially, the head-positioning systems of the hard disk drives (HDDs) or the visual servo systems of robot manipulators belong to this category, because the sampling rates of measurement are relatively slow.

In the servo systems of HDDs, the head position is detected by the discrete servo signals embedded in the disks, as shown in Fig. 2. Therefore, the output sampling period T_y is decided by the number of these signals and the rotational frequency of the spindle motor. However, it is possible to set the control period T_u shorter than T_y because of the recent development of CPU. Thus, the controller can be regarded as the multirate system which have the hardware restriction of $T_u < T_y$.

In the head-positioning control of HDD, the control strategy is divided into two modes: seeking mode and following mode. In the track-seeking mode, the feedforward performance is important because the head is

☆ Provisionally accepted for special section on developments in high precision servo systems.

*Corresponding author. Tel.: +81-47-9556; fax: +81-47-9500.

E-mail addresses: fujimoto@vos.nagaokaut.ac.jp (H. Fujimoto), hori@hori.t.u-tokyo.ac.jp (Y. Hori).

0967-0661/02/$ - see front matter
PII: S0967-0661(02)00010-2

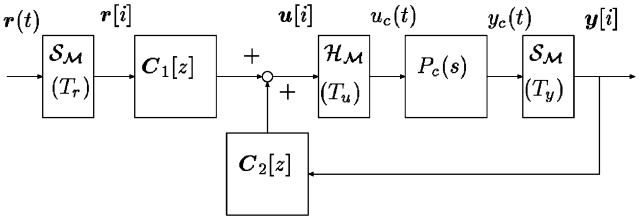

Fig. 1. Two-degree-of-freedom control system.

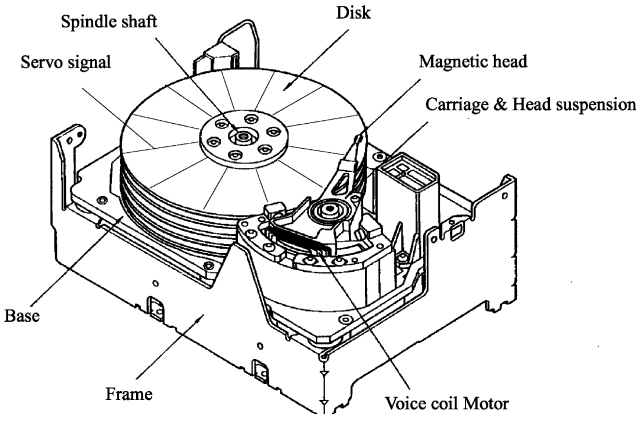

Fig. 2. Hard disk drive.

moved to the desired track as fast as possible. After that, the head needs to be positioned on the desired track while the information is read or written. In the track-following mode, the disturbance rejection performance is important because the head is positioned precisely on the desired track under the vibrations generated by disk rotation and other disturbances. In this paper, the proposed TDOF controllers are applied to each mode.

For HDDs, multirate controllers have demonstrated higher performance in both feedforward (Takakura, 1999; Kobayashi et al., 1998) and feedback (Chiang, 1990; Hara & Tomizuka, 1999) characteristics. This paper applies the proposed perfect tracking controller to the track-seeking mode, and the proposed perfect disturbance rejection controller is also applied to the track-following mode.

2. Design of the multirate TDOF controller

In this section, new multirate TDOF controllers are proposed. For the restriction of $T_u < T_y$, the frame period T_f is defined as $T_f = T_y$ (Araki, 1993), and the dynamics of the controller is described by T_f. In the proposed multirate scheme, the plant input is changed N times during T_f and the plant state is evaluated M times in this interval as shown in Fig. 3. The positive integers M and N are referred to as input and state multiplicities, respectively. N is determined by the hardware restriction. The state multiplicity is defined as $M = N/n$, where n is the plant order.

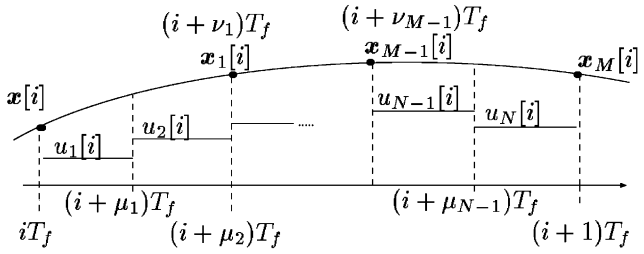

Fig. 3. Multirate sampling control.

In Fig. 3, μ_j $(j = 0, 1, \ldots, N)$ and v_k $(k = 1, \ldots, M)$ are the parameters for the timing of the input changing and the state evaluation, which satisfy conditions (1) and (2).

$$0 = \mu_0 < \mu_1 < \mu_2 < \cdots < \mu_N = 1, \tag{1}$$

$$0 < v_1 < v_2 < \cdots < v_M = 1. \tag{2}$$

If T_y is divided at same intervals, the parameters are set to $\mu_j = j/N, v_k = k/M$.

For simplification, the continuous-time plant is assumed to be a SISO system. The proposed methods, however, can be extended to deal with the MIMO system in the same way as Fujimoto et al. (1999a).

2.1. Plant discretization by multirate sampling

Consider the continuous-time plant described by

$$\dot{\boldsymbol{x}}(t) = \boldsymbol{A}_c\boldsymbol{x}(t) + \boldsymbol{b}_c u(t), \quad y(t) = \boldsymbol{c}_c\boldsymbol{x}(t). \tag{3}$$

The discrete-time plant discretized by the multirate sampling control (Fig. 3) becomes

$$\boldsymbol{x}[i+1] = \boldsymbol{A}\boldsymbol{x}[i] + \boldsymbol{B}\boldsymbol{u}[i], \quad y[i] = \boldsymbol{C}\boldsymbol{x}[i], \tag{4}$$

where $\boldsymbol{x}[i] = \boldsymbol{x}(iT)$, and where matrices $\boldsymbol{A}, \boldsymbol{B}, \boldsymbol{C}$ and vectors $\boldsymbol{u}$ are given by

$$\left[\begin{array}{c|c} \boldsymbol{A} & \boldsymbol{B} \\ \hline \boldsymbol{C} & \boldsymbol{O} \end{array}\right] \triangleq \left[\begin{array}{c|ccc} \mathrm{e}^{\boldsymbol{A}_c T_f} & \boldsymbol{b}_1 & \cdots & \boldsymbol{b}_N \\ \hline \boldsymbol{c}_c & 0 & \cdots & 0 \end{array}\right], \tag{5}$$

$$\boldsymbol{b}_j \triangleq \int_{(1-\mu_j)T_f}^{(1-\mu_{(j-1)})T_f} \mathrm{e}^{\boldsymbol{A}_c\tau}\boldsymbol{b}_c \,\mathrm{d}\tau, \quad \boldsymbol{u} \triangleq [u_1, \ldots, u_N]^{\mathrm{T}}. \tag{6}$$

The inter-sample plant state at $t = (i + v_k)T_f$ is represented by

$$\tilde{\boldsymbol{x}}[i] = \tilde{\boldsymbol{A}}\boldsymbol{x}[i] + \tilde{\boldsymbol{B}}\boldsymbol{u}[i], \tag{7}$$

$$[\,\tilde{\boldsymbol{A}} \mid \tilde{\boldsymbol{B}}\,] \triangleq \left[\begin{array}{c|ccc} \tilde{\boldsymbol{A}}_1 & \tilde{\boldsymbol{b}}_{11} & \cdots & \tilde{\boldsymbol{b}}_{1N} \\ \vdots & \vdots & & \vdots \\ \tilde{\boldsymbol{A}}_M & \tilde{\boldsymbol{b}}_{M1} & \cdots & \tilde{\boldsymbol{b}}_{MN} \end{array}\right], \tag{8}$$

$$\tilde{\boldsymbol{A}}_k \triangleq \mathrm{e}^{\boldsymbol{A}_c v_k T_f}, \quad \tilde{\boldsymbol{x}} \triangleq [\boldsymbol{x}_1^{\mathrm{T}}, \ldots, \boldsymbol{x}_M^{\mathrm{T}}]^{\mathrm{T}}, \tag{9}$$

$$\boldsymbol{x}_k[i] = \boldsymbol{x}[i + v_k] = \boldsymbol{x}((i + v_k)T_f), \tag{10}$$

$$\tilde{\boldsymbol{b}}_{kj} \triangleq \begin{cases} \mu_j < v_k, & \int_{(v_k-\mu_j)T_f}^{(v_k-\mu_{(j-1)})T_f} \mathrm{e}^{\boldsymbol{A}_c\tau}\boldsymbol{b}_c \,\mathrm{d}\tau, \\ \mu_{(j-1)} < v_k \leqslant \mu_j, & \int_{0}^{(v_k-\mu_{(j-1)})T_f} \mathrm{e}^{\boldsymbol{A}_c\tau}\boldsymbol{b}_c \,\mathrm{d}\tau, \\ v_k \leqslant \mu_{(j-1)}, & 0. \end{cases} \tag{11}$$

2.2. Design of perfect tracking controller

In the conventional digital tracking control systems, it is impossible to track the desired trajectory with zero error (Tomizuka, 1987), because the discrete-time plant discretized by the zero-order-hold usually has unstable zeros (Åström, Hangander, & Sternby, 1984).

The unstable zeros problems of the discrete-time plant have been resolved by zero assignment method in the use of multirate control in Kabamba (1987) and Mita, Chida, Kazu, and Numasato (1990). However, Moore, Bhattacharyya, and Dahleh (1993) showed that those methods sometimes had disadvantages of large overshoot and oscillation in the inter-sample points because the control input changed back and forth very quickly. On the other hand, authors proposed perfect tracking control by introducing the multirate feedforward control, which never has this problem because all of the plant states are controlled along the smoothed desired trajectories (Fujimoto et al., 2001; Fujimoto, Hori, & Kawamura, 1999b). In this section, perfect tracking controller $\boldsymbol{C}_1[z]$ is designed so that the plant state ($\boldsymbol{x}$) completely tracks the desired trajectory ($\boldsymbol{x}^*$) at every sampling points $T_r(= T_y/M)$.

The control law of Fig. 1 is described by

$$\boldsymbol{u} = \boldsymbol{C}_1\boldsymbol{r} + \boldsymbol{C}_2\boldsymbol{y} \tag{12}$$

$$= \boldsymbol{F}\hat{\boldsymbol{x}} + \boldsymbol{Q}\boldsymbol{e}_y + \boldsymbol{K}\boldsymbol{r}, \tag{13}$$

where $\boldsymbol{K}, \boldsymbol{Q} \in \boldsymbol{RH}_\infty$ are free parameters (Zhou, Doyle, & Glover, 1996; Fujimoto et al., 2001). Therefore, Fig. 1 can be transferred to Fig. 4. In the figure, $\mathscr{H}_M$, $\mathscr{S}$, and the thick lines represent the multirate hold, the sampler, and the multirate signals, respectively. In this paper, $\boldsymbol{K}$ becomes a constant matrix.

Because the estimation errors of the observer become zero ($\hat{\boldsymbol{x}} = \boldsymbol{x}, \boldsymbol{e}_y = 0$) for the nominal plant, from (7) and (13), this system is represented by

$$\tilde{\boldsymbol{x}}[i] = (\tilde{\boldsymbol{A}} + \tilde{\boldsymbol{B}}\boldsymbol{F})\boldsymbol{x}[i] + \tilde{\boldsymbol{B}}\boldsymbol{K}\boldsymbol{r}[i]. \tag{14}$$

Because the non-singularity of the matrix $\tilde{\boldsymbol{B}}$ is proved in Araki and Hagiwara (1986), the coefficient matrices of (14) can be arbitrary assigned by $\boldsymbol{F}$ and $\boldsymbol{K}$. In this paper, the parameters $\boldsymbol{F}$ and $\boldsymbol{K}$ can be selected so that the following equations are satisfied:

$$\tilde{\boldsymbol{A}} + \tilde{\boldsymbol{B}}\boldsymbol{F} = \boldsymbol{O}, \quad \tilde{\boldsymbol{B}}\boldsymbol{K} = \boldsymbol{I}. \tag{15}$$

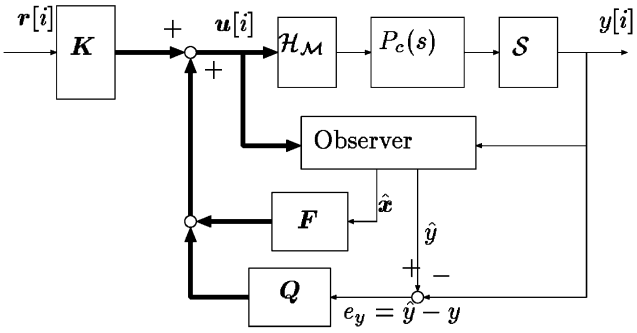

Fig. 4. Basic structure of TDOF control.

From (15), $\boldsymbol{F}$ and $\boldsymbol{K}$ are given by

$$\boldsymbol{F} = -\tilde{\boldsymbol{B}}^{-1}\tilde{\boldsymbol{A}}, \quad \boldsymbol{K} = \tilde{\boldsymbol{B}}^{-1}. \tag{16}$$

Therefore, (14) is described by $\tilde{\boldsymbol{x}}[i] = \boldsymbol{r}[i]$. Utilizing the inter-sample desired state $\tilde{\boldsymbol{x}}^*[i]$, if the reference input is set to $\boldsymbol{r}[i] = \tilde{\boldsymbol{x}}^*[i]$, we find that perfect tracking ($\tilde{\boldsymbol{x}}[i] = \tilde{\boldsymbol{x}}^*[i]$) can be achieved at every sampling point T_r.

Because $\boldsymbol{C}_1[z]$ of (12) can be transferred to (17), $\boldsymbol{C}_1[z]$ is given by

$$\boldsymbol{C}_1[z] = (\boldsymbol{M} - \boldsymbol{C}_2\boldsymbol{N})\boldsymbol{K}, \tag{17}$$

$$\boldsymbol{M} = \left[\begin{array}{c|c} \boldsymbol{A} + \boldsymbol{B}\boldsymbol{F} & \boldsymbol{B} \\ \hline \boldsymbol{F} & \boldsymbol{I} \end{array}\right] = \boldsymbol{I} + z^{-1}\boldsymbol{F}\boldsymbol{B},$$

$$\boldsymbol{N} = \left[\begin{array}{c|c} \boldsymbol{A} + \boldsymbol{B}\boldsymbol{F} & \boldsymbol{B} \\ \hline \boldsymbol{C} & \boldsymbol{O} \end{array}\right] = z^{-1}\boldsymbol{C}\boldsymbol{B} \tag{18}$$

as shown in Fig. 5, where $\boldsymbol{M}$ and $\boldsymbol{N}$ are the right coprime factorization of the plant $\boldsymbol{P}[z] = \boldsymbol{N}\boldsymbol{M}^{-1}$ (Sugie & Yoshikawa, 1986; Fujimoto et al., 2001). The initial state variable of (18) is set to be identical with the initial plant state $\boldsymbol{x}[0]$. The internal stability of the proposed control system is guaranteed because $\boldsymbol{M}, \boldsymbol{N} \in \boldsymbol{RH}_\infty$.

Next, it is shown that the structure of perfect tracking controller is very simple and clear. Fujimoto et al. (2001) showed that the structure of the proposed controller was represented in Fig. 6. The plant $\boldsymbol{P}[z]$ is driven by the stable inverse system. When the tracking error $e[i]$ is generated by disturbance or modeling error, the feedback controller $\boldsymbol{C}_2[z]$ works in order to compensate the error $e[i]$. Thus, $\boldsymbol{C}_2[z]$ must be a robust controller which renders the sensitivity function $\boldsymbol{S}[z] = (\boldsymbol{I} - \boldsymbol{P}[z]\boldsymbol{C}_2[z])^{-1}$ sufficiently small at the frequency of the desired trajectory. The reason is that the sensitivity function $\boldsymbol{S}[z]$ represents variation of the command response $\boldsymbol{G}_{yr}[z]$ under the variation of $\boldsymbol{P}[z]$ (Sugie & Yoshikawa, 1986).

2.3. Design of perfect disturbance rejection controller

In this section, novel multirate feedback controller is proposed based on the state space design of the

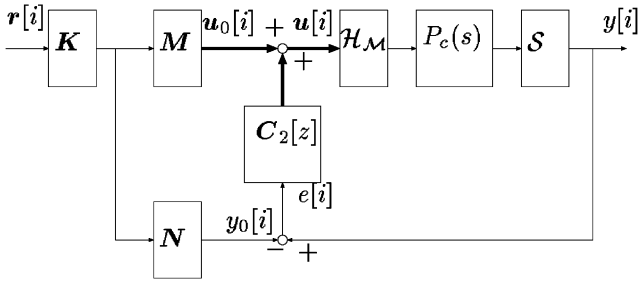

Fig. 5. Implementation of the proposed controller.

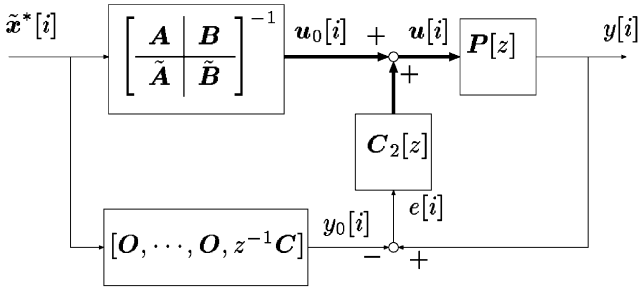

Fig. 6. Structure of the proposed controller.

disturbance observer (Ohnishi, Shibata, & Murakami, 1996).

Consider the continuous-time plant model described by

$$\dot{\boldsymbol{x}}_p(t) = \boldsymbol{A}_{cp}\boldsymbol{x}_p(t) + \boldsymbol{b}_{cp}(u(t) - d(t)), \tag{19}$$

$$y(t) = \boldsymbol{c}_{cp}\boldsymbol{x}_p(t), \tag{20}$$

where $d(t)$ is the disturbance input. Let the disturbance model be

$$\dot{\boldsymbol{x}}_d(t) = \boldsymbol{A}_{cd}\boldsymbol{x}_d(t), \quad d(t) = \boldsymbol{c}_{cd}\boldsymbol{x}_d(t). \tag{21}$$

For example, the step-type disturbance can be modeled by $\boldsymbol{A}_{cd} = 0, \boldsymbol{c}_{cd} = 1$. The continuous-time augmented system consisting of (19) and (21) is represented by

$$\dot{\boldsymbol{x}}(t) = \boldsymbol{A}_c\boldsymbol{x}(t) + \boldsymbol{b}_c u(t), \tag{22}$$

$$y(t) = \boldsymbol{c}_c\boldsymbol{x}(t), \tag{23}$$

$$\boldsymbol{A}_c \triangleq \begin{bmatrix} \boldsymbol{A}_{cp} & -\boldsymbol{b}_{cp}\boldsymbol{c}_{cd} \\ \boldsymbol{O} & \boldsymbol{A}_{cd} \end{bmatrix}, \quad \boldsymbol{b}_c \triangleq \begin{bmatrix} \boldsymbol{b}_{cp} \\ \boldsymbol{0} \end{bmatrix}, \quad \boldsymbol{x} \triangleq \begin{bmatrix} \boldsymbol{x}_p \\ \boldsymbol{x}_d \end{bmatrix},$$

$$\boldsymbol{c}_c \triangleq [\boldsymbol{c}_{cp}, \boldsymbol{0}].$$

Discretizing (22) by the multirate sampling control, the inter-sample plant state at $t = (i + v_k)T_f$ can be calculated from the kth row of (7) by

$$\boldsymbol{x}[i + v_k] = \tilde{\boldsymbol{A}}_k\boldsymbol{x}[i] + \tilde{\boldsymbol{B}}_k\boldsymbol{u}[i], \tag{24}$$

$$\tilde{\boldsymbol{A}}_k = \begin{bmatrix} \tilde{\boldsymbol{A}}_{pk} & \tilde{\boldsymbol{A}}_{pdk} \\ \boldsymbol{O} & \tilde{\boldsymbol{A}}_{dk} \end{bmatrix}, \quad \tilde{\boldsymbol{B}}_k = \begin{bmatrix} \tilde{\boldsymbol{B}}_{pk} \\ \boldsymbol{O} \end{bmatrix}.$$

For plant (22) discretized by (4), the discrete-time observer on the sampling points is obtained from Gopinath's method by

$$\hat{\boldsymbol{v}}[i + 1] = \hat{\boldsymbol{A}}\hat{\boldsymbol{v}}[i] + \hat{\boldsymbol{b}}y[i] + \hat{\boldsymbol{J}}\boldsymbol{u}[i], \tag{25}$$

$$\hat{\boldsymbol{x}}[i] = \hat{\boldsymbol{C}}\hat{\boldsymbol{v}}[i] + \hat{\boldsymbol{d}}y[i]. \tag{26}$$

As shown in Fig. 7, let the feedback control law be

$$\boldsymbol{u}[i] = \boldsymbol{F}_p\hat{\boldsymbol{x}}_p[i] + \boldsymbol{F}_d\hat{\boldsymbol{x}}_d[i] = \boldsymbol{F}\hat{\boldsymbol{x}}[i], \tag{27}$$

where $\boldsymbol{F} \triangleq [\boldsymbol{F}_p, \boldsymbol{F}_d]$. Notice that the $\boldsymbol{F}$ of the above equation is different from that of (13) used in $\boldsymbol{C}_1[z]$ design. Letting $\boldsymbol{e}_v$ be the estimation errors of the observer ($\boldsymbol{e}_v = \hat{\boldsymbol{v}} - \boldsymbol{v}$), the following equation is obtained:

$$\hat{\boldsymbol{x}}[i] = \boldsymbol{x}[i] + \hat{\boldsymbol{C}}\boldsymbol{e}_v[i]. \tag{28}$$

From (24) to (28), the closed-loop system is represented by

$$\begin{bmatrix} \boldsymbol{x}_p[i + v_k] \\ \boldsymbol{x}_d[i + v_k] \\ \boldsymbol{e}_v[i + 1] \end{bmatrix} = \begin{bmatrix} \tilde{\boldsymbol{A}}_{pk} + \tilde{\boldsymbol{B}}_{pk}\boldsymbol{F}_p & \tilde{\boldsymbol{A}}_{pdk} + \tilde{\boldsymbol{B}}_{pk}\boldsymbol{F}_d & \tilde{\boldsymbol{B}}_{pk}\boldsymbol{F}\hat{\boldsymbol{C}} \\ \boldsymbol{O} & \tilde{\boldsymbol{A}}_{dk} & \boldsymbol{O} \\ \boldsymbol{O} & \boldsymbol{O} & \hat{\boldsymbol{A}} \end{bmatrix} \times \begin{bmatrix} \boldsymbol{x}_p[i] \\ \boldsymbol{x}_d[i] \\ \boldsymbol{e}_v[i] \end{bmatrix}. \tag{29}$$

Because full row rank of the matrix $\tilde{\boldsymbol{B}}_{pk}$ can be assured (Araki & Hagiwara, 1986), $\boldsymbol{F}_d$ can be selected so that the (1,2) element of the above equation becomes zero for all $k = 1, \ldots, M$.

$$\tilde{\boldsymbol{A}}_{pdk} + \tilde{\boldsymbol{B}}_{pk}\boldsymbol{F}_d = \boldsymbol{O}. \tag{30}$$

The simultaneous equation of (30) for all k becomes

$$\tilde{\boldsymbol{A}}_{pd} + \tilde{\boldsymbol{B}}_p\boldsymbol{F}_d = \boldsymbol{O}, \tag{31}$$

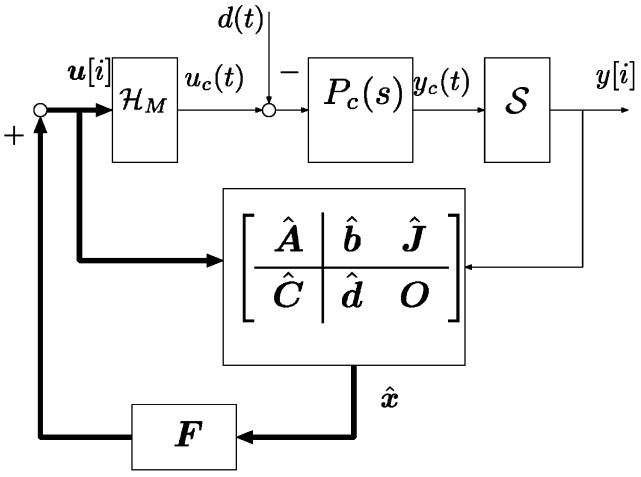

Fig. 7. Multirate control with disturbance observer.

$$\left[\tilde{\boldsymbol{A}}_{pd} \mid \tilde{\boldsymbol{B}}_p\right] \triangleq \left[\begin{array}{c|c} \tilde{\boldsymbol{A}}_{pd1} & \tilde{\boldsymbol{B}}_{p1} \\ \vdots & \vdots \\ \tilde{\boldsymbol{A}}_{pdM} & \tilde{\boldsymbol{B}}_{pM} \end{array}\right]. \tag{32}$$

From (31), $\boldsymbol{F}_d$ is obtained by

$$\boldsymbol{F}_d = -\tilde{\boldsymbol{B}}_p^{-1}\tilde{\boldsymbol{A}}_{pd}. \tag{33}$$

In (29) and (30), the influence of disturbance $\boldsymbol{x}_d[i]$ on the inter-sample state $\boldsymbol{x}_p[i+v_k]$ at $t=(i+v_k)T_f$ can become zero. Moreover, $\boldsymbol{x}_p[i]$ and $\boldsymbol{e}_v[i]$ at the sampling point converge to zero at the rate of the eigenvalues of $\tilde{\boldsymbol{A}}_{pM}+\tilde{\boldsymbol{B}}_{pM}\boldsymbol{F}_p$ and $\hat{\boldsymbol{A}}$ (the poles of the regulator and observer). Therefore, perfect disturbance rejection is achieved ($\boldsymbol{x}_p[i+v_k]=0$) in the steady state. The poles of the regulator and observer will be tuned by the tradeoff between the performance and stability robustness.

Substituting (25) into (27), the feedback-type controller is obtained by

$$\begin{bmatrix} \hat{\boldsymbol{v}}[i+1] \\ \boldsymbol{u}[i] \end{bmatrix} = \begin{bmatrix} \hat{\boldsymbol{A}}+\hat{\boldsymbol{J}}\boldsymbol{F}\hat{\boldsymbol{C}} & \hat{\boldsymbol{b}}+\hat{\boldsymbol{J}}\boldsymbol{F}\hat{\boldsymbol{d}} \\ \boldsymbol{F}\hat{\boldsymbol{C}} & \boldsymbol{F}\hat{\boldsymbol{d}} \end{bmatrix} \begin{bmatrix} \hat{\boldsymbol{v}}[i] \\ y[i] \end{bmatrix}. \tag{34}$$

Because the multirate system becomes multi-input system, the feedback gain $\boldsymbol{F}_p$ cannot be decided uniquely only by the pole assignment of the regulator ($\tilde{\boldsymbol{A}}_{pM}+\tilde{\boldsymbol{B}}_{pM}\boldsymbol{F}_p$). In Fujimoto, Hori, Yamaguchi, and Nakagawa (1999c), authors have developed the inter-sample observer, which can utilize this redundancy effectively. The advantage of this observer is that the stability margin is increased by compensating the long delay of the holder.

3. Applications to HDD

3.1. Modeling of the plant

In this section, the proposed methods are applied to a 3.5-in hard disk drive. Let the nominal model of this plant be

$$P_c(s) = \frac{K_f K_a}{M_p s^2}\,\mathrm{e}^{-sT_d}. \tag{35}$$

The parameters of this plant are shown in Table 1. While servo signals are detected at a constant period of about 138 μs, the control input can be changed 4 times. Therefore, the proposed approach is applicable. In (35), the time delay $T_d = T_{calc} + T_{equiv}$ is considered, where T_{calc} is the calculation delay of the processor, and T_{equiv} is the equivalent delay of the current control and the notch filter for the second mechanical resonance mode. Therefore, the proposed method has extended to systems with time delay in Fujimoto, Hori, Yamaguchi, and Nakagawa (2000) and Fujimoto, (2000).

Table 1
Parameters of the plant

Amplifier gain	K_a	1.996	A/V
Force constant	K_f	2.95	N/A
Mass	M_p	6.983	g
Track pitch	T_p	3.608	μm/trk
Sampling time	T_s	138.54	μs
Calculation delay	T_{calc}	38	μs
Equivalent delay	T_{equiv}	38.7	μs
Input multiplicity	N	4	

3.2. Applications of perfect tracking controller to seeking mode

In this section, perfect tracking control proposed in Section 2.2 is applied to the seeking mode. The actual plant has the first mechanical resonance mode around 2.7 kHz. The Nyquist frequency is also 3.6 kHz. In spite of those, the target seeking time is set to 3 sampling time (2.4 kHz) for one track seeking in these experiments.

Perfect tracking controller is designed on input multiplicity $N=4$. Because the plant is a second-order system ($n=2$), perfect tracking is assured $N/n=2$ times during the sampling period. In the following simulations and experiments, the proposed method is compared with ZPETC proposed in Tomizuka (1987). ZPETC is one of the most well-known and important feedforward controllers in the mechanical system control. Kobayashi et al. (1998) and Yi and Tomizuka (1999) applied it to hard disk drive control.

The control period T_u of ZPETC becomes four times as long as that of the proposed method because ZPETC is a single-rate controller[1] and two methods are compared at the same sampling period T_y.[2] The feedback controllers of two methods are same single-rate PI-lead filters. Moreover, the desired trajectory (36) is selected, which jerk (differential acceleration) is smooth in order not to excite the mechanical resonance mode.

$$y^*(s) = \frac{A_r}{s(\tau_r s+1)^4}. \tag{36}$$

The parameters of these desired trajectories are shown in Table 2. In these experiments, the feedforward inputs $\boldsymbol{u}_0[i]$ and $y_0[i]$ in Figs. 5 and 6 are obtained by off-line calculation in order to save the processor resources. Therefore, the order of the feedforward controller and the desired trajectory are not related to the calculation time delay.

[1] Kobayashi et al. (1998) and Gu and Tomizuka (1999) attempt to extend ZPETC to multirate controllers.

[2] In Fujimoto et al. (2001), the proposed perfect tracking controller is compared with ZPETC in the same control period T_u for the position control system of servomotor, which has no sampling restriction (i.e. $T_y = T_u$).

Fig. 8 shows simulation and experimental results of condition A (1 trk). Fig. 8(a) and (b) shows that the proposed method gives better performance than ZPETC. While the response of ZPETC has large tracking error caused by the unstable zero, that of the proposed method has almost zero tracking error. Fig. 8(c) also indicates that the proposed multirate input is very smooth. Fig. 8(d) shows that the seeking time of the proposed method gets to about 3 sampling times in the experiments.

Table 2
Parameters of the trajectories

	A_r (trk)	f_r $(= 1/2\pi\tau_r)$ (kHz)
Condition A	1	2.8
Condition B	6	1.7

The frequency responses from the desired trajectory $y_d[i]$ to the output $y[i]$ are shown in Fig. 9, which includes the preview action (Tomizuka, 1987). Because the proposed method (PTC) assures perfect tracking, the command response becomes 1 in all frequencies. However, the gain of ZPETC decreases in the high frequency. The frequency of the short-span seeking is around 2 kHz. Therefore, the proposed method has advantages in seeking control.

Table 3 shows the average seeking time which is measured in the 2000 times experiments. The seeking time is defined as the time from which the seeking starts to the point when the remaining distance becomes less than 0.4 μm and the overshoot is less than 0.4 μm. The seeking time of the proposed method (PTC) is much smaller than that of ZPETC and the conventional settling control (Yamaguchi, Numasato, & Hirai, 1998). In the short-span seeking (1 trk), the seeking time of the

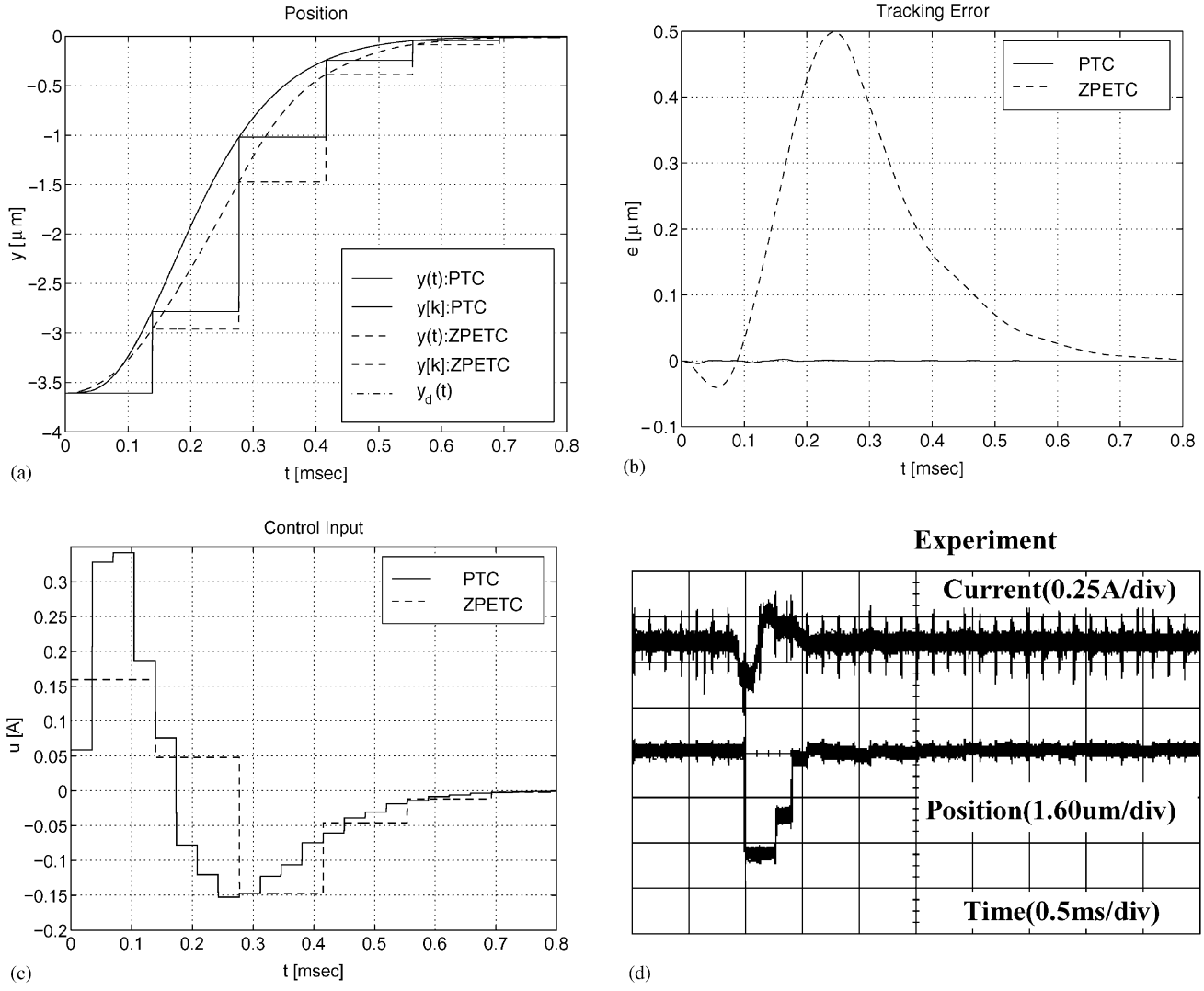

Fig. 8. Simulation and experimental results of the seeking mode (1 trk seeking): (a) position (Simulation); (b) error (Simulation); (c) control input (Simulation); (d) experiment.

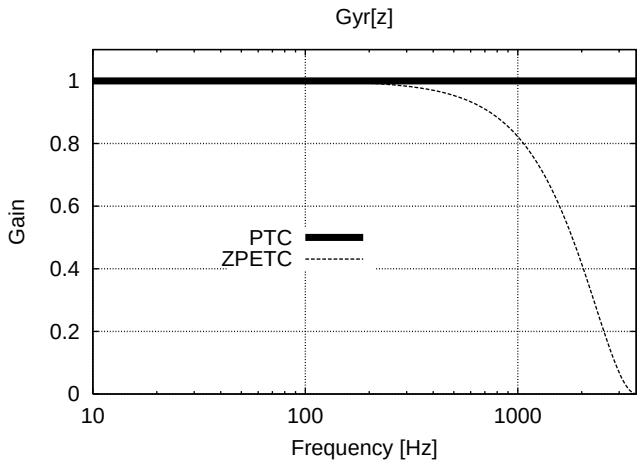

Fig. 9. Frequency responses ($y[z]/y^*[z]$).

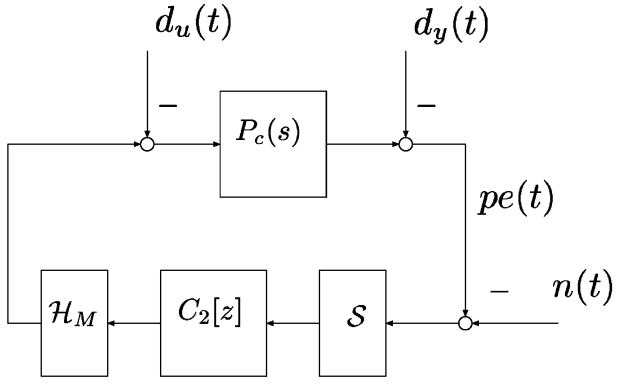

Fig. 10. Following mode.

Table 3
Average seeking-time on experiments

	PTC (ms)	ZPETC (ms)	Conventional (ms)
A 1 trk	0.4394 ($3.17T_s$)	0.5226 ($3.77T_s$)	0.5738 ($4.14T_s$)
B 6 trk	1.200 ($8.66T_s$)	1.325 ($9.57T_s$)	1.933 ($14.0T_s$)

proposed method is 19% and 31% shorter than the ZPETC and conventional method, respectively. In the middle-span seeking (6 trk), the proposed method is 1 and 6 sampling times faster. The details of these experiments have been presented in Fujimoto et al. (2000).

Furthermore, the proposed method also has great advantages in the systems such as NC machines or robots, where the tracking error for the desired trajectory is much important. In Fujimoto et al. (2001), perfect tracking control is applied to the position control system for servomotor, which shows that the tracking error is much improved not only at the sampling points but also in the inter-sample points on the experiments.

3.3. Applications of perfect disturbance rejection controller to the following mode

In this section, perfect disturbance rejection control system proposed in Section 2.3 is applied to the following mode. The block diagram of the following mode is shown in Fig. 10. The disturbance $d_y(t)$ represents vibration of the track generated by disk rotation, which is known as track runout. The objective of this mode is to keep the position error $pe(t)$ zero. $n(t)$ and $d_u(t)$ represent measurement noise and acceleration disturbance, respectively.

In the following mode, two kinds of disturbance should be considered: repeatable and non-repeatable runout. Repeatable runout (RRO) is synchronous with the disk rotation, and non-repeatable runout (NRRO) is asynchronous. There exist several approaches to reject RRO (Kempf, Messner, Tomizuka, & Horowitz, 1993). In this paper, the RRO is modeled by a sinusoidal disturbance, and it is perfectly rejected at M inter-sample points in the steady state.

In this paper, the following disturbance models are considered:

$$\text{(A): } d(s) = \frac{1}{s(s^2+\omega_R^2)}, \quad \text{(B): } d(s) = \frac{1}{s}. \tag{37}$$

The model (A) makes the sensitivity function $S(s)$ small at low frequencies and the rotation frequency of the disk $\omega_R(=2\pi 120)$. The model (B) is introduced for comparison with conventional PI-lead filters, because the controller consisting of state-feedback and disturbance observer for (B) becomes the second order with an integrator.

Perfect disturbance rejection controllers are designed with $N=2$ and 4. The proposed method is compared with the single-rate disturbance observer, in which the disturbance is modeled by $d[z]=Z[d(s)]$. The poles of the regulator and observer are assigned to set the open loop 0 dB cross-over to about 500 Hz. Fig. 11(a) shows the sensitivity and complimentary sensitivity functions ($S[z]$ and $T[z]$) for model (A) and (B). The SISO closed-loop transfer functions are obtained at the output of plant. It is found that the proposed controllers have the internal model of (37).

Fig. 11(b) and (c) shows the simulation results for a 120 Hz sinusoidal runout added from $t=0$, whose amplitude is 1 trk = 3.6 μm. Although the position

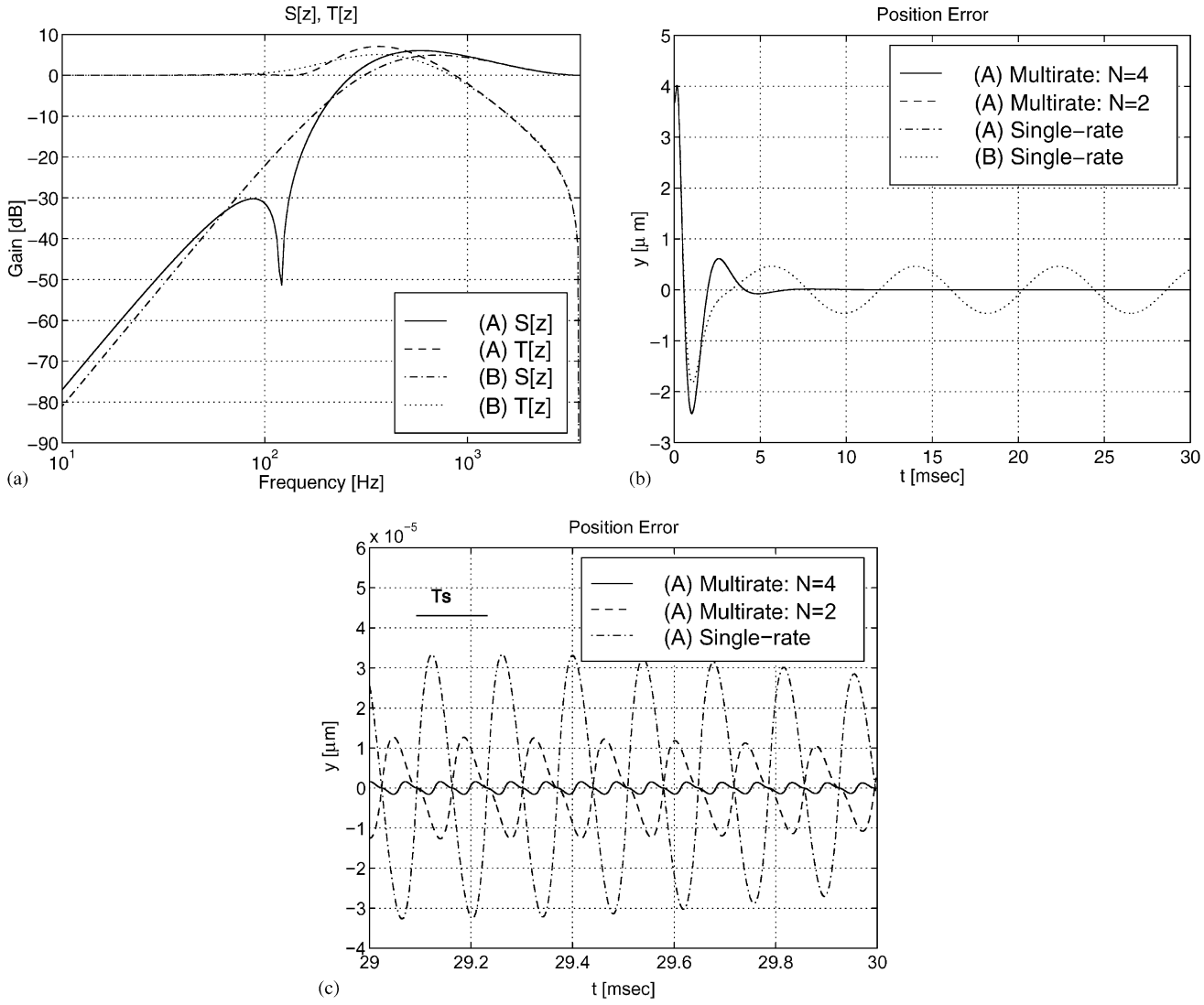

Fig. 11. Simulation results of the following mode: (a) $S[z]$ and $T[z]$; (b) position error; (c) position error in steady state.

errors are large in the transient state, the errors of the controllers (A) become zero at sampling point in the steady state, because the feedback controllers have the internal model of the disturbance. However, Fig. 11(c) shows that the inter-sample responses have errors even in the steady state. It is shown that the errors of the plant position and velocity become zero at every $2T_s/N$ by the proposed controllers. Moreover, the inter-sample position errors of the proposed multirate methods are much smaller than that of the single-rate controller.

In the above simulations, only the first mode of RRO is considered. However, in Fujimoto and Hori (2000), this method is extended to repetitive disturbance rejection control in order to deal with the high-order RRO. Moreover, the proposed approaches are applied to the visual servo system for robot manipulators, and the effectiveness is verified through simulations and experiments (Fujimoto & Hori, 2001).

4. Conclusion

In this paper, the digital control systems which have hardware restrictions of $T_u < T_y$ were assumed, the multirate feedforward controller was proposed, which assured perfect tracking at M inter-sample points. Next, the multirate feedback controller was also proposed, which guaranteed perfect disturbance rejection at M inter-sample points in the steady state.

Furthermore, the former was applied to the track-seeking mode of hard disk drive, and the later was also applied to the track-following mode. The advantages of

these approaches were demonstrated by the simulations and experiments.

Acknowledgements

Finally, the authors wish to thank Dr. Takashi Yamaguchi and Mr. Shinsuke Nakagawa of Hitachi, Ltd. for cooperation in conducting experiments and for many helpful discussions.

References

Araki, M. (1993). Recent developments in digital control theory. In *Twelvth IFAC world congress.* Sydney, Vol. 9 (pp. 251–260).

Araki, M., & Hagiwara, T. (1986). Pole assignment by multirate-data output feedback. *International Journal of Control*, *44*(6), 1661–1673.

Åström, K. J., Hangander, P., & Sternby, J. (1984). Zeros of sampled system. *Automatica*, *20*(1), 31–38.

Chiang, W. W. (1990). Multirate state-space digital controller for sector servo systems. In *IEEE Conference on decision control.* CDC90, Honolulu (pp. 1902–1907).

Fujimoto, H. (2000). *General framework of multirate sampling control and applications to motion control systems.* Ph.D. thesis, The University of Tokyo.

Fujimoto, H., & Hori, Y. (2000). Vibration suppression and optimal repetitive disturbance rejection control in semi-Nyquist frequency region using multirate sampling control. In *IEEE Conference on decision control.* CDC2000, Sydney (pp. 691–700).

Fujimoto, H., & Hori, Y. (2001). Visual servoing based on intersample disturbance rejection by multirate sampling control—time delay compensation and experimental verification. In *IEEE Conference on decision control* number TuA11-6, in preparation.

Fujimoto, H., Hori, Y., & Kawamura, A. (1999b). High performance perfect tracking control based on multirate feedforward/feedback controllers with generalized sampling periods. In *14th IFAC world congress*, Vol. C. IFAC99, Beijing (pp. 61–66).

Fujimoto, H., Hori, Y., & Kawamura, A. (2001). Perfect tracking control based on multirate feedforward control with generalized sampling periods. *IEEE Transaction Industrial Electronics*, *48*(3), 636–644.

Fujimoto, H., Hori, Y., Yamaguchi, T., & Nakagawa, S. (1999c). Proposal of perfect tracking and perfect disturbance rejection control by multirate sampling and applications to hard disk drive control. In *IEEE Conference on decision control.* CDC99, Pheonix (pp. 5277–5282).

Fujimoto, H., Hori, Y., Yamaguchi, T., & Nakagawa, S. (2000). Proposal of seeking control of hard disk drives based on perfect tracking control using multirate feedforward control. In *IEEE International workshop on advanced motion control* (pp. 74–79).

Fujimoto, H., Kawamura, A., & Tomizuka, M. (1999a). Generalized digital redesign method for linear feedback system based on *N*-delay control. *IEEE/ASME Transaction on Mechatronics*, *4*(2), 101–109.

Gu, Y., & Tomizuka, M. (1999). High performance tracking control system under measurement constraints by multirate control. In *14th IFAC world congress*, Vol. C. IFAC99, Beijing (pp. 67–71).

Hara, T., & Tomizuka, M. (1999). Performance enhancement of multi-rate controller for hard disk drives. *IEEE Transaction on Magnetics*, *35*(2), 898–903.

Kabamba, P. T. (1987). Control of linear systems using generalized sampled-data hold functions. *IEEE Transaction on Automatic Control*, *32*(9), 772–783.

Kempf, C., Messner, W., Tomizuka, M., & Horowitz, R. (1993). Comparison of four discrete-time repetitive algorithms. *IEEE Control System Magazine*, *13*(5), 48–54.

Kobayashi, M., Yamaguchi, T., Oshimi, I., Soyama, Y., Hara, Y., & Hirai, H. (1998). Multirate zero phase error feedforward control for magnetic disk drives. In *JSME, IIP '98* (pp. 21–22) (in Japanese).

Mita, T., Chida, Y., Kazu, Y., & Numasato, H. (1990). Two-delay robust digital control and its applications—avoiding the problem on unstable limiting zeros. *IEEE Transaction on Automatic Control*, *35*(8), 962–970.

Moore, K. L., Bhattacharyya, S. P., & Dahleh, M. (1993). Capabilities and limitations of multirate control schemes. *Automatica*, *29*(4), 941–951.

Ohnishi, K., Shibata, M., & Murakami, T. (1996). Motion control for advanced mechatronics. *IEEE/ASME Transaction on Mechatronics*, *1*(1), 56–67.

Sugie, T., & Yoshikawa, T. (1986). General solution of robust tracking problem in two-degree-of-freedom control systems. *IEEE Transaction on Automatic Control*, *31*(6), 552–554.

Takakura, S. (1999). Design of the tracking system using *N*-delay two-degree-of-freedom control and its application to hard disk drives. In *IEEE conference on control applications.* CCA99, Kohala Coast (Hawaii) (pp. 170–175).

Tomizuka, M. (1987). Zero phase error tracking algorithm for digital control. *ASME. Journal of Dynamic System Measurement and Control*, *109*, 65–68.

Yamaguchi, T., Numasato, H., & Hirai, H. (1998). A mode-switching control for motion control and its application to disk drives: Design of optimal mode-switching conditions. *IEEE/ASME Transaction on Mechatronics*, *3*(3), 202–209.

Yi, L., & Tomizuka, M. (1999). Two-degree-of-freedom control with robust feedback control for hard disk servo systems. *IEEE/ASME Transaction on Mechatronics*, *4*(1), 17–24.

Zhou, K., Doyle, J., & Glover, K. (1996). *Robust and optimal control.* Englewood Cliffs, NJ: Prentice-Hall.